High-resolution particle spectroscopy of 186Re

Wheldon, Carl; Ashwood, Nicholas; Curtis, Neil; Freer, Martin; Munoz-Britton, T; Ziman, Victor; Faestermann, T; Wirth, HF; Hertenberger, R; Lutter, R; Gernhäuser, R; Krücken, R; Maier, L

DOI:
10.1088/0954-3899/36/9/095102

Document Version
Publisher's PDF, also known as Version of record

Citation for published version (Harvard):
Wheldon, C, Ashwood, N, Curtis, N, Freer, M, Munoz-Britton, T, Ziman, V, Faestermann, T, Wirth, HF, Hertenberger, R, Lutter, R, Gernhäuser, R, Krücken, R & Maier, L 2009, 'High-resolution particle spectroscopy of 186Re', Journal of Physics G: Nuclear and Particle Physics, vol. 36, no. 9, 095102, pp. 1-11. https://doi.org/10.1088/0954-3899/36/9/095102

J. Phys. G: Nucl. Part. Phys. **36** (2009) 095102 (11pp) doi:10.1088/0954-3899/36/9/095102

High-resolution particle spectroscopy of ^{186}Re

C Wheldon[1], N I Ashwood[1], N Curtis[1], M Freer[1], T Munoz-Britton[1], V A Ziman[1], T Faestermann[2], H-F Wirth[3], R Hertenberger[3], R Lutter[3], R Gernhäuser[2], R Krücken[2] and L Maier[2]

[1] School of Physics and Astronomy, University of Birmingham, Edgbaston, Birmingham, B15 2TT, UK
[2] Physik Department, Technische Universität München, D-85748 Garching, Germany
[3] Sektion Physik, Ludwig-Maximilians-Universität München, D-85748 Garching, Germany

E-mail: c.wheldon@bham.ac.uk

Received 20 May 2009
Published 24 July 2009
Online at stacks.iop.org/JPhysG/36/095102

Abstract
The transfer reaction $^{187}_{75}$Re(p, d)$^{186}_{75}$Re has been studied using the Munich Q3D spectrograph at a proton bombarding energy of 21 MeV. The excitation energy regime up to ≈2.5 MeV has been elucidated, over 30 states observed for the first time and a precision down to 0.5 keV achieved. Blocked BCS calculations are presented, in excellent agreement with the experimentally observed low-lying structures in ^{186}Re. These calculations have been used to predict the structures of the strongly populated states above 1 MeV, and 4-quasiparticle configurations are suggested.

1. Introduction

The odd–odd rhenium isotopes ($Z = 75$) close to the valley of β stability are interesting for several reasons. Rhenium lies at the proton-rich edge of the well-deformed transition region, beyond which the nuclei begin to exhibit shape changes such as triaxiality and reduced prolate deformations that eventually lead to the spherical nucleus $^{208}_{82}$Pb. Furthermore, the nuclear levels exhibit a wealth of structure at low excitation energies due to the high-level density and the proximity of high-Ω single-particle orbitals to the Fermi surfaces for both protons and neutrons. (Ω is the projection of angular momentum on to the nuclear symmetry axis and $K = \sum_i \Omega_i$ over i single quasiparticles.) This latter aspect can lead to half-lives for low-lying levels significantly longer than those of the ground states for several isotopes including ^{186}Re in the present study, but also ^{184,190}Re. For example, a $K^\pi = (8^+)$ state at 149 ± 7 keV in ^{186}Re has a lifetime of 2.0×10^5 y [1] in contrast to the $K^\pi = 1^-$ ground state which lives for only 3.7183(11) d [2]. The excitation energy of the isomer is inferred from x-ray yields and despite several studies, outlined below, the ground state remains the only level with a firm spin and parity assignment. Earlier transfer reaction studies could not resolve states closer than

≈5 keV and extended only up to 900 keV, though some (n, γ) studies have probed low-spin states to 2.2 MeV [2]. The present experiment is sufficient to populate levels beyond the pair gap and can easily resolve states 4 keV apart. The latter point is particularly important due to the large density of states.

The present work uses a high-resolution Q3D spectrograph and focal-plane detector coupled with an intense beam to populate states in ^{186}Re up to ≈2.5 MeV with high precision.

2. Experimental method

A 21 MeV, 270 nA proton beam from the tandem Van de Graaf accelerator of the Maier-Leibnitz-Laboratory of LMU and TU Munich was used to bombard a thin target of ^{187}Re comprising 70 μg cm^{-2} of ^{187}Re backed by 8.2 μg cm^{-2} of carbon. The ≈15 MeV deuteron ejectiles were analysed by the Q3D magnetic spectrograph [3] set at $\theta = 35^\circ$ with a horizontal acceptance of $\pm 3^\circ$. The acceptance at a given magnet setting is approximately 10% of the ejectile energy, i.e. ≈1.5 MeV. A beam pipe was mounted at 0° out of the back of the chamber enabling the beam dump to be located ≈80 cm downstream from the target position. This restricted the Q3D angle to a minimum of 35°. The optical properties of the spectrograph mean that ejectiles of a given energy are focused to the same point on the focal plane, independent of angle, meaning that focal-plane position corresponds to excitation energy. Three Q3D settings were measured centred at $E_x^{\mathrm{Q3D}} = 400$, 1500 and 2000 keV. The focal-plane detector [4] comprises a plastic scintillator and horizontal wires to measure energy/energy loss, followed by 255 vertical wires for position. This allows particles to be distinguished via their mass-to-charge ratio. The master trigger for this study required a coincidence between the plastic scintillator and a horizontal wire. The primary reaction, $^{187}_{75}$Re(p, d)$^{186}_{75}$Re, has $Q_0 = -5.13$ MeV, whereas reactions on ^{12}C and ^{16}O contaminants in the target have $Q_0 = -16.50$ and -13.44 MeV respectively and therefore have insufficient energy to appear at the focal plane. Reactions on the other stable isotope of rhenium, ^{185}Re, would populate states in ^{184}Re, the structure of which is well known [5]. Reactions on ^{185}Re have $Q_0 = -5.44$ MeV, thereby leading to a shift of 310(4) keV in the direction of higher excitation energies for peaks in ^{184}Re, with respect to ^{186}Re. No evidence is observed for states in ^{184}Re implying a target purity >99%.

3. Results

The final position spectrum from the focal plane was constructed by fitting a symmetric Gaussian peak shape to those vertical-wire positions above threshold, event by event and taking the centroid. This was done using bespoke software [7]. The peaks in the final spectra (e.g. figure 1) were fitted using the RadWare analysis package [8] using a symmetric Gaussian and a Gaussian convoluted with an exponential function to reproduce the non-symmetric peak shapes. For the Q3D focal plane, an 'internal calibration' was used for which energies of known states up to 900 keV were used, primarily those from ^{185}Re(n, γ) reactions with relatively small uncertainties [2]. A weighted polynomial fit of order 2 was performed for the first Q3D setting at $E_x^{\mathrm{Q3D}} = 400$ keV. From this, energies up to ≈1.2 MeV could be assigned. The energy overlap between successive Q3D settings meant that the higher excitation energies could be calibrated by 'boot-strapping' using energies from the first setting. Clearly this technique leads to increased uncertainties on the energies for settings 2 and 3 which is reflected in the tabulated results of table 1, summarizing the levels in ^{186}Re.

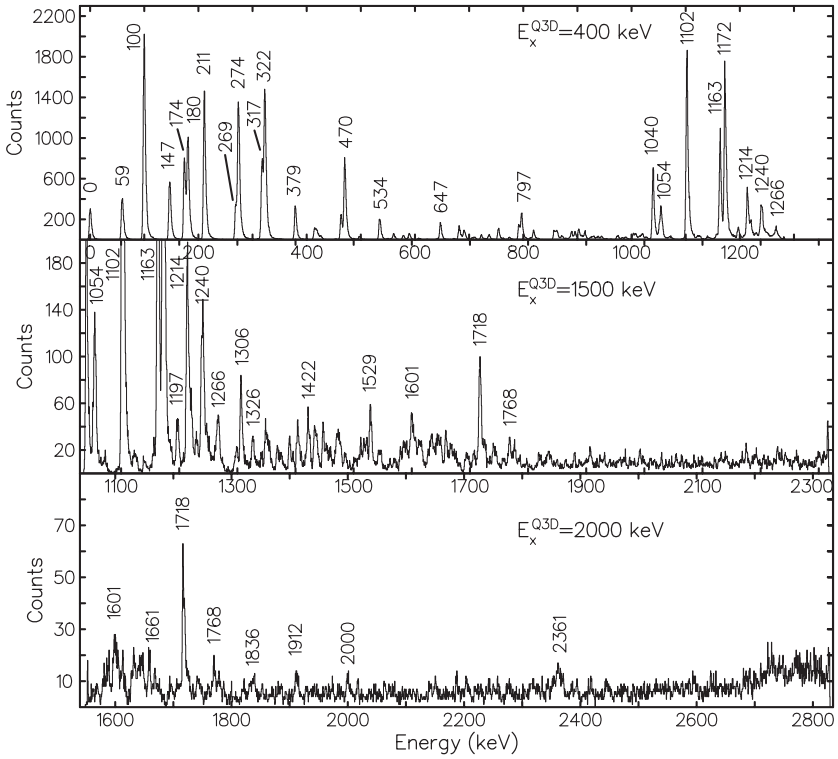

Figure 1. Spectra from the Q3D focal plane with three different settings: (top) $E_x^{\mathrm{Q3D}} = 400$ keV, (middle) $E_x^{\mathrm{Q3D}} = 1500$ keV, (bottom) $E_x^{\mathrm{Q3D}} = 2000$ keV.

In the present work several energies have been determined to a higher accuracy than previously known and over 30 levels have been newly observed (see table 1), all of which lie above 400 keV. Furthermore, this is the first time that results from a (p, d) reaction leading to ^{186}Re have been reported, and for several levels, the improved accuracy stems from the different population of levels as well as the increased resolution. In general, the negative parity states are populated most strongly, due to the positive parity states containing either a $\frac{9}{2}^-$ proton or a high-j neutron, neither of which are favoured in neutron pick-up with a proton beam. Neutron removal from the ^{187}Re target preferentially leads to negative parities based on the $\frac{5}{2}^+[402]$ proton and the neutron Fermi surface lies between the juxtaposed $\frac{1}{2}^-[510]$ and $\frac{3}{2}^-[512]$ orbitals and the $\frac{7}{2}^-[503]$ orbitals, leading to strong population of these configurations.

Based on the tentative spin assignments in [2], the intensity is greatest for most rotational bands at $I = 3\hbar$ (the ^{187}Re ground-state spin is $I = \frac{5}{2}\hbar$). The measurement at only one angle restricts the amount of data that can be extracted in terms of spin and parity characteristics of the final states, however, the intensities are in broad agreement with that expected based on the tentative assignments from the systematic evaluation presented in [2]. Furthermore, the tentative multi-quasiparticle assignments [2] for the ground state, $K^\pi = (3)^-$ (100 keV) and $(6)^-$ (180 keV), all show a consistency with their strong population intensity observed in the current work as do their complementary couplings: $K^\pi = (4)^-$ (174 keV), $(2)^-$ (211 keV) and $(1)^-$ (317 keV). $K^\pi = (1)^+$ (602 keV), $(3)^+$ (314 keV and 351), $(4)^+$ (471 keV),

Table 1. Energies and intensities measured in the present work. The deviation from the published values are quoted, ΔE ($= E_{\text{present}} - E_{\text{lit.}}$). The final column details the configurations tentatively assigned in [2]. Where no value for ΔE is given the state is assumed to be observed for the first time, implying that there are no known levels within the uncertainties. All known states up to 1.1 MeV are included; thereafter, only levels observed in this work. 'Doublet?' refers to the state labelled and the one in the row above.

Energies	ΔE	$E_{\text{lit.}}$ [a]	Intensity	I^{π} [a]	K^{π} [a]	Tent. config.[a]		
	(keV)		(arb.)	$\hbar$		π	$\otimes$	ν
0.0	0.0	0.0	2947(65)	1^-	1^-	$\frac{5}{2}^+[402]$	–	$\frac{3}{2}^-[512]$
59.0(5)	−0.01	59.010(3)	4209(75)	$(2)^-$	1^-	$\frac{5}{2}^+[402]$	–	$\frac{3}{2}^-[512]$
99.6(5)	+0.24	99.361(3)	19 274(150)	$(3)^-$	3^-	$\frac{5}{2}^+[402]$	+	$\frac{1}{2}^-[510]$
146.7(5)	+0.43	146.274(4)	5832(95)	$(3)^-$	1^-	$\frac{5}{2}^+[402]$	–	$\frac{3}{2}^-[512]$
–		≈149	–	(8^+)	8^+	$\frac{5}{2}^+[402]$	–	$\frac{11}{2}^+[615]$
173.9(5)	−0.03	173.929(4)	7983(100)	$(4)^-$	4^-	$\frac{5}{2}^+[402]$	+	$\frac{3}{2}^-[512]$
180.1(5)		≈186	9026(160)	$(6)^-$	6^-	$\frac{5}{2}^+[402]$	+	$\frac{7}{2}^-[503]$
210.5(5)	−0.20	210.699(5)	13 661(433)	$(2)^-$	2^-	$\frac{5}{2}^+[402]$	–	$\frac{1}{2}^-[510]$
268.8(5)	0.00	268.798(6)	3455(169)	$(4)^-$	1^-	$\frac{5}{2}^+[402]$	–	$\frac{3}{2}^-[512]$
273.5(5)	−0.09	273.627(5)	12 669(683)	$(4)^-$	3^-	$\frac{5}{2}^+[402]$	+	$\frac{1}{2}^-[510]$
–		314.009(5)	–	$(3)^+$	3^+	$\frac{5}{2}^+[402]$	–	$\frac{11}{2}^+[615]$
317.4(5)	+0.94	316.463(12)	7834(314)	$(1)^-$	1^-	$\frac{5}{2}^+[402]$	–	$\frac{7}{2}^-[503]$
Doublet?	−0.45	317.845(7)		$(5)^-$	4^-	$\frac{5}{2}^+[402]$	+	$\frac{3}{2}^-[512]$
322.4(5)	+0.02	322.379(6)	12 941(256)	$(3)^-$	2^-	$\frac{5}{2}^+[402]$	–	$\frac{1}{2}^-[510]$
–		≈330	–	$(5)^+$	5^+	$\frac{9}{2}^-[514]$	+	$\frac{1}{2}^-[510]$
–		351.202(16)	–	$(3)^+$	$(3)^+$	$\frac{9}{2}^-[514]$	–	$\frac{3}{2}^-[512]$
378.6(5)	+0.21	378.392(12)	3095(113)	$(2)^-$	1^-	$\frac{5}{2}^+[402]$	–	$\frac{7}{2}^-[503]$
414.9(5)		–	1158(82)		–			
418.7(5)	−0.91	417.792(8)	670(56)	$(5)^-$	1^-	$\frac{5}{2}^+[402]$	–	$\frac{3}{2}^-[512]$
–		420.559(7)	–	$(4)^+$	3^+	$\frac{5}{2}^+[402]$	–	$\frac{11}{2}^+[615]$
425.4(5)	−0.42	425.823(7)	322(29)	$(2^+, 3^+, 4^+)$	–			
463.3(5)	+0.33	462.969(9)	2267(60)	$(5)^-$	3^-	$\frac{5}{2}^+[402]$	+	$\frac{1}{2}^-[510]$
470.0(5)	+0.22	469.779(17)	7003(110)	$(4)^-$	2^-	$\frac{5}{2}^+[402]$	–	$\frac{1}{2}^-[510]$
Doublet?	−0.51	470.514(13)		$(3)^-$	1^-	$\frac{5}{2}^+[402]$	–	$\frac{7}{2}^-[503]$
–		≈471	–	$(4)^+$	4^+	$\frac{9}{2}^-[514]$	–	$\frac{1}{2}^-[510]$
496.7(10)	−0.59	497.293(10)	155(24)	$(6)^-$	4^-	$\frac{5}{2}^+[402]$	+	$\frac{3}{2}^-[512]$
498.9(10)	−1.82	500.722(16)	86(23)	$(4)^+$	$(3)^+$	$\frac{9}{2}^-[514]$	–	$\frac{3}{2}^-[512]$
533.8(15)	−0.57	534.37(4)	1021(89)	$(4)^-$	–			
549.5(10)	+0.17	549.330(9)	42(15)	$(^+)$	–			
560.4(10)	+0.42	559.976(9)	300(38)	$(5)^+$	3^+	$\frac{5}{2}^+[402]$	–	$\frac{11}{2}^+[615]$
563.1(10)		≈562	111(21)	$(6)^+$	6^+	$\frac{9}{2}^-[514]$	+	$\frac{3}{2}^-[512]$
578.3(10)	+0.58	577.723(16)	385(31)	(2^-)	2^-	$\frac{5}{2}^+[402]$	–	$\frac{9}{2}^-[505]$
589.2(10)	+0.49	588.709(13)	537(35)	(4^-)	1^-	$\frac{5}{2}^+[402]$	–	$\frac{7}{2}^-[503]$
–		601.58(3)	–	$(1)^+$	1^+	$\frac{9}{2}^-[514]$	–	$\frac{7}{2}^-[503]$
606.8(10)		–	74(20)		–			

Table 1. (Continued.)

Energies	ΔE	$E^{a}_{lit.}$	Intensity	$I^{\pi\ a}$	$K^{\pi\ a}$	Tent. config.[a]		
	(keV)		(arb.)	$\hbar$		π	$\otimes$	ν
610.1(10)		–	52(12)		–			
–		623.89(6)	–	(1^-)	–			
646.8(10)	+0.47	646.332(19)	1340(61)	(5^-)	2^-	$\frac{5}{2}^+[402]$	–	$\frac{1}{2}^-[510]$
–		657.99(3)	–	$(2)^+$	1^+	$\frac{9}{2}^-[514]$	–	$\frac{7}{2}^-[503]$
–		665.188(18)	–	$(5)^+$	$(3)^+$	$\frac{9}{2}^-[514]$	–	$\frac{3}{2}^-[512]$
681.4(10)	+1.37	680.03(15)	984(60)	$(2^-, 3^-)$	–			
686.5(15)	+0.44	686.058(17)	154(34)	(3^-)	2^-	$\frac{5}{2}^+[402]$	–	$\frac{9}{2}^-[505]$
690.3(10)	+1.0	689.3	672(44)	(1^-)	–			
Doublet?	−1.04	691.34(15)		(6^-)	3^-	$\frac{5}{2}^+[402]$	+	$\frac{1}{2}^-[510]$
705.7(15)		–	137(18)	–	–			
710.2(15)		–	174(22)	–	–			
722.4(10)		–	327(25)	–	–			
728.2(15)		–	83(16)	–	–			
736.5(10)	+0.37	736.127(15)	384(26)	(5^-)	1^-	$\frac{5}{2}^+[402]$	–	$\frac{7}{2}^-[503]$
–		744.81(5)	–	$(3)^+$	1^+	$\frac{9}{2}^-[514]$	–	$\frac{7}{2}^-[503]$
753.9(10)	+0.2	753.7	905(67)	$(2^-, 3^-)$	–			
762.1(15)	+0.32	761.42(19)	87(22)	$(1^-, 2^-, 3^-)$	–			
774.2(15)		–	111(48)	–	–			
–		785.31(20)	–	–	–			
791.8(10)	+0.3	791.5	1296(63)	(1^-)	–			
796.6(10)	+0.03	796.63(20)	1963(78)	$(\leqslant 3)$	–			
–		803(10)	–		–			
813.6(15)	+1.4	812.2	112(28)	(1^-)	–			
818.6(10)	−0.34	818.94(19)	712(68)	$(2^-, 3^-)$	–			
–		821.31(6)	–	$(\leqslant 3)$	–			
–		826.152(18)	–	(4^-)	2^-	$\frac{5}{2}^+[402]$	–	$\frac{9}{2}^-[505]$
–		855.04(5)	–	(4^+)	1^+	$\frac{9}{2}^-[514]$	–	$\frac{7}{2}^-[503]$
857.0(10)	−0.9	857.9	876(57)	$(2^-, 3^-)$	–			
861.2(10)	−2.97	864.17(15)	676(45)	$(2^-, 3^-)$	–			
871.0(10)	−0.3	871.3	270(27)	$(-)$	–			
888.8(15)	+0.4	888.4	431(48)	(4^-)	–			
Doublet?	−1.0	889.8		$(1^-, 2^-, 3^-)$	–			
895.3(15)	+0.3	895.0	331(43)	$(2^-, 3^-, 4^-)$	–			
902.4(15)	+0.6	901.8	623(59)	$(2^-, 3^-)$	–			
913.5(15)	−0.1	913.6	452(50)	$(2^-, 3^-)$	–			
926.8(15)	+3.1	923.7	100(57)	$(2^-, 3^-)$	–			
929.6(15)	−0.4	930.0	178(74)	$(^-)$	–			
937.4(15)	+1.9	935.5	173(79)	$(2^-, 3^-)$	–			
Doublet?	−0.9	938.3		(1^-)	–			
944.5(15)	−1.9	946.4	185(73)	$(2^-, 3^-)$	–			
953.3(20)	−0.7	954(4)	24(40)	–	–			
973.8(15)	−1.2	975.0	484(158)	$(^-)$	–			
982.9(15)		–	204(77)	–	–			

Table 1. (Continued.)

Energies	ΔE	$E^{a}_{lit.}$	Intensity	$I^{\pi\ a}$	$K^{\pi\ a}$	Tent. config.[a]		
	(keV)		(arb.)	$\hbar$		π	$\otimes$	ν
988.8(15)	0.0	988.8	269(92)	–	–			
–		997.84(6)	–	(5^+)	1^+	$\frac{9}{2}^-[514]$	–	$\frac{7}{2}^-[503]$
–		999.3	–	$(2^-, 3^-, 4^-)$	–			
1003.2(20)	−1.6	1004.8	339(170)	$(2^-, 3^-, 4^-)$	–			
1007.4(20)		–	273(97)		–			
1016.9(20)	+1.9	1015.0	90(99)	$(2^-, 3^-, 4^-)$	–			
1019.7(20)	+0.3	1019.4	267(167)	$(1^-, 2^-, 3^-)$	–			
1027.2(20)		–	69(62)		–			
1039.6(5)	−0.3	1039.9	4871(92)	$(2^-, 3^-, 4^-)$	–			
–		1042.9	–	(1^-)	–			
–		1046.9	–	$(2^-, 3^-, 4^-)$	–			
1050.7(15)		–	1102(120)		–			
1054.1(10)	+0.8	1053.4	2228(65)	$(1^-, 2^-, 3^-)$	–			
–		1057.1	–	$(2^-, 3^-)$	–			
1070.6(15)	+0.8	1069.8	237(35)	$(2^-, 3^-)$	–			
–		1073.3	–	$(2^-, 3^-)$	–			
–		1097.1	–	(4^-)	–			
1101.9(5)	−1.0	1102.9	16428(146)	$(2^-, 3^-)$	–			
1157.1(10)	−0.5	1157.6	405(42)	$(2^-, 3^-, 4^-)$	–			
1163.1(5)	+0.1	1163.0	8720(416)	(1^-)	–			
1172.3(5)	−1.3	1173.6	14686(689)	$(^-)$	–			
1196.7(10)	−0.4	1097.1	731(47)	$(2^-, 3^-)$	–			
1213.9(10)		–	4110(152)	–	–			
1219.5(10)	+0.4	1219.1	1152(144)	(1^-)	–			
1229.7(15)		–	215(56)	–	–			
1239.8(10)		–	3072(569)	–	–			
1266.4(10)		–	783(154)	–	–			
1298.1(15)	+0.6	1297.5	180(19)	$(1^-, 2^-, 3^-)$	–			
1306.4(10)	−1.1	1307.5	692(39)	$(^-)$	–			
1326.5(10)		–	246(27)	–	–			
1341.6(20)		–	83(19)	–	–			
1349.1(15)		–	357(31)	–	–			
1354.0(15)	−1.2	1355.2	151(24)	$(2^-, 3^-)$	–			
1369.2(15)		–	216(25)	–	–			
1375.4(15)	+0.3	1375.1	106(23)	$(1^-, 2^-, 3^-)$	–			
1390.5(15)		–	273(28)	–	–			
1404.3(10)	+1.1	1403.2	408(35)	(1^-)	–			
Doublet?	−1.5	1405.8		$(2^-, 3^-, 4^-)$	–			
1421.7(10)		–	479(36)	–	–			
1434.2(20)	−2.8	1437(4)	442(36)	–	–			
1448.6(20)	−1.5	1450.1	378(32)	$(1^-, 2^-, 3^-)$	–			
1458.7(20)	+0.6	1458.1	149(24)	$(2^-, 3^-)$	–			
1472.7(20)		–	478(33)	–	–			
1485.6(20)	−3.4	1489(5)	102(21)	–	–			

Table 1. (Continued.)

Energies	ΔE	$E^{a}_{lit.}$	Intensity	I^{π} [a]	K^{π} [a]	Tent. config.[a]
	(keV)		(arb.)	$\hbar$		$\pi \otimes \nu$
1512.7(20)		–	153(28)	–	–	
1520.5(20)		–	242(31)	–	–	
1529.4(20)	−2.0	1531.4	475(42)	$(2^-, 3^-)$	–	
1545.1(20)	+0.1	1545.0	140(27)	$(^-)$	–	
1587.1(20)		–	305(38)	–	–	
1601.4(20)		–	638(107)	–	–	
1613.8(20)		–	354(80)	–	–	
1633.8(20)		–	425(53)	–	–	
1646.0(20)	+2.1	1643.9	452(45)	–	–	
Doublet?	−2.1	1648.1		–	–	
1660.6(20)	−1.5	1662.1	225(18)	$(^-)$	–	
1694.9(20)	−1.6	1696.5	149(33)	$(2^-, 3^-)$	–	
1707.6(20)		–	228(27)	–	–	
1717.6(15)	−1.5	1719.1	886(104)	$(2^-, 3^-, 4^-)$	–	
1742.4(20)		–	606(44)	–	–	
1768.4(20)	+0.4	1768(5)	309(94)	–	–	
1776.4(20)		–	307(70)	–	–	
1907.3(20)	+1.3	1906(4)	325(35)	–	–	
2000(4)	−5	2005(4)	224(47)	–	–	
2321(4)		–	550(67)	–	–	
2361(4)		–	1258(90)	–	–	

[a] Reference [2].

$(5)^+$ (330 keV), $(6)^+$ (563 keV) and $(8)^+$ (149 keV) are all absent, as expected, having peak areas of $\lesssim$50 counts.

The ≈186 keV doublet [2] is measured here as 180.1(5) keV with no significant second component present. This energy is in agreement with earlier (d, p) and (d, t) reactions reporting 180(2) and 177(2), respectively [9]. It is through this state that higher lying positive-parity states such as the ≈330, ≈471 and ≈562 keV levels decay. See table 2 for details of specific configurations.

The pair of states at 414.9(5) and 418.7(5) keV is also noteworthy. The 414.9 keV state is the lowest lying previously unobserved state, most likely due to its proximity to the 418.7 keV level, the latter of which is assigned as the $I^{\pi} = (5)^-$ level of the ground-state band [2]. The 414.9 keV state is relatively strongly populated and may correspond to the first excited state of the $K^{\pi} = (6)^-$ level at 180 keV, i.e. an $I^{\pi} = 7^-$ level. The intensity is consistent with such a placement and the energy separation between the first two levels (=235 keV) is similar to that for the same configuration in ^{184}Re (=219 keV) [5].

Above 1 MeV a significant number of states appear that are strongly populated, many of which are observed here for the first time. The 1 MeV excitation energy suggests that these states are likely to be built on 4-quasiparticle configurations. Taking the most intense of these states and constructing regular sequences give rise to two possible series: 1054.1, 1101.9, 1163.1, 1239.8, 1326.5 keV and 1172.3, 1213.9, 1266.4 keV which may correspond to new band structures.

In order to calculate the configurations in this excitation energy regime, blocked BCS multi-quasiparticle configurations have been performed of the type developed by Jain *et al* [10]. Pairing strengths of $G_\nu = 21.5/A$ and $G_\pi = 23.1/A$ MeV have been used, consistent with those for the close-lying isotopes $^{184}_{74}$W [11] and $^{184}_{75}$Re [5]. Deformation parameters of $\varepsilon_2 = 0.198$ and $\varepsilon_4 = 0.058$ are used from [12] ($\beta_2 = 0.218$ and $\beta_4 = -0.053$ from solving the equations in [13]). The single-particle energies for the orbitals close to the Fermi surface were fitted to reproduce the known single-quasiparticle energies in ^{185}W [14] and ^{187}Os [15, 16] for neutrons and ^{185}Re [14, 16] and ^{187}Re [15] for protons. For each particle type, the averaged single-particle energies were used. Protons and neutrons are treated independently in the calculations. The results are shown in table 2 where the calculated energies, $E_{\rm calc}$, comprise the multi-quasiparticle energies, $E_{\rm mqp}$, and the residual nucleon–nucleon interaction energies, $E_{\rm res}$. The latter are taken from empirical data [17, 18]. As can be seen, the calculated energies are in good agreement with the energies of configurations assigned in [2, 19] with the discrepancies all being less than 100 keV and in most cases <70 keV.

In addition, for the ground-state, 1^- band: $\nu 3/2^-[512]-\pi 5/2^+[402]$ and 3^- band: $\nu 1/2^-[510]+\pi 5/2^+[402]$, the g-factors extracted using the rotational model expressions [20] and the published γ-ray branching ratios [2] are in good agreement with the assigned configurations. Examining the configurations in table 2 around 1 MeV suggests that 4-quasiparticle configurations can indeed account for the intense population seen in the $E_x^{\rm Q3D} = 1500$ keV spectrum of figure 1. In particular, the 1^- state calculated at 1100 keV and the 3^- state at 996 keV are the most plausible candidates for the observed structures, have low spins and are built on the favoured orbitals: $\nu : 1/2^-[510], 3/2^-[512], 7/2^-[503]$ and $\pi : 5/2^+[402]$. These energies tie in well with those observed: 1054 and 1172 keV.

The $K^\pi = (8^+)$ isomer is calculated here at 226 keV, compared to the deduced energy of ≈149 keV. The assignment of this configuration to the isomer seems reasonable, and the fact that it lies below the $K^\pi = 6^-$ level at 180 keV can account for the extremely long, 2.0×10^5 y half-life. The only levels lying lower in excitation energy have spins of 1–3, leading to, in the most favourable case, an $E5$ decay to the 100 keV state. This high multipolarity coupled with the low decay energy of ≈50 keV leads to the long lifetime. Note that a competing β^--decay branch to ^{186}Os has not been ruled out, but is constrained to <10% of the intensity [1].

The 180 keV level has a proposed $K^\pi = (6)^-$ configuration [2] compatible with its population here given the orbitals involved, namely $\nu\frac{7}{2}^-[503] \otimes \pi\frac{5}{2}^+[402]$ which, as noted earlier, are expected to be strongly populated. No de-excitations have been reported from this state, but only six opportunities exist. A 6 keV K-allowed $E2$ to the $K^\pi = (4)^-$ level is one possibility. Alternatives include a direct decay to the $K^\pi = (8^+)$ isomer via a ≈30 keV K-allowed $M2$ transition, a twice K-forbidden 33 keV $M3$ transition to the 147 keV level, an 80 keV K-allowed $M3$ decay to the 100 keV state or 121 ($E4$) and 180 keV ($M5$) decays to the 59 keV and ground-state levels respectively. All of these paths are hindered, either due to low energies or due to high multipolarities leading to a significant half-life for the 180 keV level. Brandi *et al* [21] have reported a 70(1) μs half-life decaying via 99 ± 6 and 128 ± 6 keV γ-rays together with intense coincident K x-rays. Seegmiller *et al* [1] echo earlier suggestions [9] that this could be associated with the ≈186 keV level. Indeed, a cursory glance suggests that the decays fit well with the newly established 180 keV excitation energy implying decays to the 100 keV and 59 keV levels respectively, with the highly converted initial 80 keV transition to the 100 keV level producing x-rays. (The decay from the 59 keV state would be obscured by the K x-ray peak, centred at 60.6 keV.) However, the Weisskopf single-particle estimates for such transitions are consistent only with half-lives of the order of hours or longer, even when taking the large electron-conversion coefficients into account. Examining the Weisskopf single-particle estimates for all six decay routes listed above, the

Table 2. Low-lying 2- and 4-quasiparticle states in $^{186}_{75}Re_{111}$ compared to experimentally observed levels. Configurations up to $10\hbar$ and 1.5 MeV are included.

	Configuration			Energy (keV)				
K^π	ν	$\otimes$	π	E_{mqp} [a]	E_{res}	E_{calc}	E_{expt}	ΔE [b]
0^+	$\frac{9}{2}^-[505]$	–	$\frac{9}{2}^-[514]$	890	−107	783	–	
0^-	$\frac{7}{2}^-[503]$	–	$\frac{7}{2}^+[404]$	958	−62	896	–	
1^-	$\frac{3}{2}^-[512]$	–	$\frac{5}{2}^+[402]$	78	−78	0	0	0
1^-	$\frac{7}{2}^-[503]$	–	$\frac{5}{2}^+[402]$	287	+96.5	384	316	−68
1^-	$\frac{11}{2}^+[615]$	–	$\frac{9}{2}^-[514]$	507	+142.5	650	–	
1^+	$\frac{7}{2}^-[503]$	–	$\frac{9}{2}^-[514]$	570	+107	677	602	−75
1^-	$-\frac{7}{2}^-[503]$, $\frac{3}{2}^-[512]$, $\frac{1}{2}^-[510]$	+	$\frac{5}{2}^+[402]$	1092	+7.5	1100	–	
1^+	$-\frac{11}{2}^+[615]$, $\frac{3}{2}^-[512]$, $\frac{1}{2}^-[510]$	+	$\frac{5}{2}^+[402]$	1156	−2.5	1153	–	
2^-	$\frac{1}{2}^-[510]$	–	$\frac{5}{2}^+[402]$	107	+55	162	211	+49
2^-	$\frac{9}{2}^-[505]$	–	$\frac{5}{2}^+[402]$	663	−74.5	589	578	−11
2^+	$\frac{9}{2}^+[624]$	–	$\frac{5}{2}^+[402]$	690	+103.5	794	–	
3^-	$\frac{1}{2}^-[510]$	+	$\frac{5}{2}^+[402]$	121	−55	66	99	+33
3^+	$\frac{3}{2}^-[512]$	–	$\frac{9}{2}^-[514]$	361	−76.5	285	351	+66
3^+	$\frac{11}{2}^+[615]$	–	$\frac{5}{2}^+[402]$	280	+124.5	405	314	−91
3^-	$\frac{7}{2}^-[503]$, $\frac{3}{2}^-[512]$, $\frac{1}{2}^-[510]$	–	$\frac{5}{2}^+[402]$	1120	−124.5	996	–	
4^-	$\frac{3}{2}^-[512]$	+	$\frac{5}{2}^+[402]$	120	+78	198	174	−24
4^+	$\frac{1}{2}^-[510]$	–	$\frac{9}{2}^-[514]$	390	+71.5	462	(≈471)	(+9)
5^+	$\frac{1}{2}^-[510]$	+	$\frac{9}{2}^-[514]$	404	−71.5	333	(≈330)	(−3)
5^+	$\frac{11}{2}^+[615]$	–	$\frac{1}{2}^+[400]$	918	N/A	–	–	
5^-	$\frac{3}{2}^-[512]$	+	$\frac{7}{2}^+[404]$	889	−52	837	–	
5^+	$\frac{11}{2}^+[615]$, $\frac{3}{2}^-[512]$, $\frac{1}{2}^-[510]$	–	$\frac{5}{2}^+[402]$	1212	−48.5	1164	–	
5^-	$\frac{7}{2}^-[503]$, $-\frac{3}{2}^-[512]$, $\frac{1}{2}^-[510]$	+	$\frac{5}{2}^+[402]$	1148	+258.5	1407	–	
6^-	$\frac{7}{2}^-[503]$	+	$\frac{5}{2}^+[402]$	287	−96.5	191	180	−11
6^+	$\frac{3}{2}^-[512]$	+	$\frac{9}{2}^-[514]$	403	+76.5	480	(≈562)	(+82)
6^+	$\frac{11}{2}^+[615]$	+	$\frac{1}{2}^+[400]$	932	N/A	–	–	
7^+	$\frac{9}{2}^+[624]$	+	$\frac{5}{2}^+[402]$	760	−103.5	657	–	
7^-	$\frac{9}{2}^-[505]$	+	$\frac{5}{2}^+[402]$	733	+74.5	808	–	
7^-	$\frac{7}{2}^-[503]$, $\frac{3}{2}^-[512]$, $-\frac{1}{2}^-[510]$	+	$\frac{5}{2}^+[402]$	1176	−151.5	1025	–	
7^+	$\frac{11}{2}^+[615]$, $-\frac{3}{2}^-[512]$, $\frac{1}{2}^-[510]$	+	$\frac{5}{2}^+[402]$	1240	−192.5	1048	–	
8^+	$\frac{11}{2}^+[615]$	+	$\frac{5}{2}^+[402]$	350	−124.5	226	≈149	+77
8^+	$\frac{7}{2}^-[503]$	+	$\frac{9}{2}^-[514]$	570	−107	463	–	
8^-	$\frac{7}{2}^-[503]$, $\frac{3}{2}^-[512]$, $\frac{1}{2}^-[510]$	+	$\frac{5}{2}^+[402]$	1190	−261.5	929	–	
9^-	$\frac{9}{2}^+[624]$	+	$\frac{9}{2}^-[514]$	1043	−71	972	–	
9^+	$\frac{9}{2}^-[505]$	+	$\frac{9}{2}^-[514]$	1016	+107	1123	–	
9^+	$\frac{11}{2}^+[615]$, $\frac{3}{2}^-[512]$, $-\frac{1}{2}^-[510]$	+	$\frac{5}{2}^+[402]$	1268	−141.5	1127	–	
10^-	$\frac{11}{2}^+[615]$	+	$\frac{9}{2}^-[514]$	633	−142.5	491	–	
10^+	$\frac{11}{2}^+[615]$, $\frac{3}{2}^-[512]$, $\frac{1}{2}^-[510]$	+	$\frac{5}{2}^+[402]$	1282	−251.5	1031	–	

[a] For non-maximal-K couplings an amount $\frac{\hbar^2}{2\Im}\Delta K$ ($\frac{\hbar^2}{2\Im} = 14$ keV, $\Delta K = K_{\mathrm{max.}} - K$) has been subtracted to account for the change in rotational energy with-respect-to the maximal-K-coupling state for which the energy, E_{mqp}, was calculated. A value of 121 keV has been added to all E_{mqp} energies so that the calculated ground-state energy is zero after taking into account the residual interaction and rotational energy terms.

[b] $\Delta E = E_{\mathrm{expt}} - E_{\mathrm{calc}}$.

most likely are the K-allowed 6 keV $E2$ transition to the $K^\pi = (4)^-$ state and the ≈30 keV $M2$ transition to the $K^\pi = (8^+)$ isomer, with partial *transition* half-life estimates of $t_{1/2}^{\text{Weiss.}} = 1.6$ and 12 μs respectively. The same configuration lies at 172 keV in ^{188}Re with a half-life of 18.6 m and decays via 2.6 and 15.9 keV $M3$ transitions [22].

Also, of note is the 2-quasiparticle, $K^\pi = 10^-$ bandhead predicted at 491 keV: $\nu\frac{11}{2}^+[615]\otimes\pi\frac{9}{2}^-[514]$. From systematics, this is close to the expected excitation energy of the $I^\pi = 9^+$ member of the $K^\pi = 8^+$ band, and could lead to the $K^\pi = 10^-$ state being an yrast trap, i.e. forced to decay via an $M2$ transition to the $K^\pi = 8^+$ isomer. Such a state would have a significant half-life. Seegmiller *et al* [1] refer to an unplaced 109 keV $M2$ transition in table 3 of [9], which could represent the decay of a 259 keV $K^\pi = 10^-$ state to the $K^\pi = (8^+)$ isomer. Also the 70 μs half-life [21], mentioned above, could be associated with the $K^\pi = 10^-$ state if produced in (γ, n) reactions at 22.5 MeV [21]. The Weisskopf single-particle estimate for a ≈100 keV K-allowed $M2$ transition is consistent with such a half-life. The same configuration lies at 917 keV in ^{184}Re [5]. A heavy-ion reaction (deep-inelastic) or a transfer reaction with a large negative Q-value would be more suited to the population of this configuration due to its relatively high angular momentum, e.g. ^{184}W(α, d)^{186}Re, $Q_0 = -14.49$ MeV. In this context, it is also worth mentioning that neither the $K^\pi = 8^+$ nor the $K^\pi = 10^-$ configurations have been identified in ^{188}Re. Both configurations contain the $\nu\frac{11}{2}^+[615]$ orbital which in this mass region lies closer to the Fermi surface as more neutrons are added. Therefore, it can be expected that in the heavier rhenium isotopes these configurations may possess even longer lifetimes and their longevity may underlie why they have so far eluded detection.

4. Summary

In summary, many states have been observed in ^{186}Re for the first time and precisions down to 0.5 keV have been achieved. The $I^\pi = (6)^-$ level through which the higher lying positive-parity structures decay has been measured here at 180 keV and its decay routes, and associated half-life discussed. The calculated energies from blocked BCS calculations are in excellent agreement with the known seniority-2 energies and low-lying 4-quasiparticle states ∼1 MeV are predicted, in correspondence with the strong population observed in the excitation spectra.

Acknowledgments

The accelerator operators are thanked for providing a stable beam. K Eppinger and M Mahgoub are thanked for helping with the set-up. We are grateful to the target maker at Munich for providing the ^{187}Re targets and A Bergmaier for the loan of electronics. C Wheldon acknowledges receipt of an STFC Advanced Research Fellowship. Tz Kokalova is thanked for discussions and commenting on the manuscript.

References

[1] Seegmiller D W, Lindner M and Meyer R A 1972 *Nucl. Phys.* A **184** 94–112
[2] Baglin Coral M 2003 *Nucl. Data Sheets* **99** 1–196
[3] Löffler M, Scheerer H J and Vonach H 1973 *Nucl. Instrum. Methods* **111** 1–12
[4] Wirth H-F in preparation
[5] Wheldon C *et al* 2005 *Nucl. Phys.* A **763** 1–30
[6] Eberth J *et al* 2001 *Prog. Part. Nucl. Phys.* **46** 389–98
[7] Wheldon C 2008 http://www.hmi.de/people/wheldon/files/munich_decoder.c
[8] Radford D C 1995 *Nucl. Instrum. Methods Phys. Res.* A **361** 297–305
[9] Lanier R G *et al* 1969 *Phys. Rev.* **178** 1919–48

[10] Jain K, Walker P M and Rowley N 1994 *Phys. Lett.* B **322** 27–32
Jain K, Burglin O, Dracoulis G D, Fabricus B, Rowley N and Walker P M 1995 *Nucl. Phys.* A **591** 61–84
[11] Wheldon C *et al* 2004 *Eur. Phys. J.* A **20** 365–9
[12] Bengtsson R, Frauendorf S and May F R 1986 *At. Data Nucl. Data Tables* **35** 15–122
[13] Bengtsson R, Dudek J, Nazarewicz W and Olanders P 1989 *Phys. Scr.* **39** 196–220
[14] Wu S-C 2005 *Nucl. Data Sheets* **106** 619–812
[15] Basunia M S 2009 *Nucl. Data Sheets* **110** 999–1238
[16] Jain A K, Sheline R K, Sood P C and Jain K 1990 *Rev. Mod. Phys.* **62** 393–509
[17] Gallagher C J and Moskowski S A 1958 *Phys. Rev.* **111** 1282–90
[18] Kondev F G 1997 *PhD Thesis* Australian National University (unpublished)
[19] Glatz J 1973 *Z. Phys.* A **265** 335–64
[20] Bohr A and Mottelson B R 1975 *Nucl. Structure* vol 2 (New York: Benjamin)
[21] Brandi K, Engelman R, Hepp V, Kluge E, Krehbiel H and Meyer-Berkhout U 1964 *Nucl. Phys.* **59** 33–55
Krehbiel H and Meyer-Berkhout U 1961 *Z. Phys.* **165** 99–120
[22] Takahashi K, McKeown M and Scharff-Goldhaber G 1964 *Phys. Rev.* **136** B18-27